Glassy dynamics of convex polyhedra

Nikos Tasios, Anjan Prasad Gantapara, and Marjolein Dijkstra

Citation: The Journal of Chemical Physics **141**, 224502 (2014); doi: 10.1063/1.4902992
View online: http://dx.doi.org/10.1063/1.4902992
View Table of Contents: http://scitation.aip.org/content/aip/journal/jcp/141/22?ver=pdfcov
Published by the AIP Publishing

Glassy dynamics of convex polyhedra

Nikos Tasios,[a] Anjan Prasad Gantapara, and Marjolein Dijkstra
Debye Institute for Nanomaterial Science, Utrecht University, Princetonplein 1, 3584 CC Utrecht, The Netherlands

(Received 3 September 2014; accepted 18 November 2014; published online 8 December 2014)

Self-assembly of polyhedral-shaped particles has attracted huge interest with the advent of new synthesis methods that realize these faceted particles in the lab. Recent studies have shown that polyhedral-shaped particles exhibit a rich phase behavior by excluded volume interactions alone; some of these particles are even alleged to show a transition to a glass phase by quenching the liquid sufficiently fast beyond the glass transition (supercooling), such that the formation of structures with long-range order is suppressed. Despite the recent progress, no study has been made on the glass formation of polyhedral-shaped particles. Here, we study the glass behavior of polyhedral particles using advanced Monte Carlo methods. We investigate the formation of a glass of monodisperse hard polyhedral-shaped particles, namely, octahedra, tetrahedra, and triangular cupola, using simulations. Finally, the fragility of these particles is determined and compared to that of a polydisperse hard-sphere system. © *2014 AIP Publishing LLC*. [http://dx.doi.org/10.1063/1.4902992]

I. INTRODUCTION

Although the glass phase has been known and studied for a very long time,[1] in reality, this metastable state has been described by many different definitions, which reflects our limited understanding. Many materials can form glasses which exhibit a variety of properties. Creating strong and low-density glasses, and glasses with various optical and electronical properties has received special interest, a pinnacle of which are metallic glasses; these are amorphous metals with remarkable toughness and small fragility, due to the absence of crystal defects.

The focus of the scientific community's attention on glasses is well warranted, because the nature of the glass transition is still poorly understood and under continuous debate up to the current day. Materials close to the glass transition show a slowing down of their dynamics and a lack of long-range order, and hence, are often compared with highly viscous fluids. Because of the extremely slow dynamics, it is hard to study the long-time behavior of glasses. The glass transition can either occur upon cooling, or compression, and is accompanied by a smooth increase in the viscosity (unlike first-order phase transitions where abrupt changes are involved). A liquid below its standard freezing point will crystallize in the presence of a seed crystal or nucleus, around which a crystal structure can form. However, in the absence of such a nucleus, the liquid phase can be maintained all the way down to the temperature where homogeneous crystal nucleation occurs. If the system is quenched sufficiently fast, such that homogeneous nucleation does not occur, an amorphous (non-crystalline) solid will form.

If a glass former is cooled from its melting temperature to its glass transition temperature T_g, it shows an increase in its relaxation time by up to 14 decades without a significant change in its structural properties, hence it is a challenge to investigate such a system experimentally, as well as theoretically. Remarkably, supercooled liquids show a very similar scaling behavior for the relaxation times for a very large variety of different liquids. Despite the efforts to study this dramatic growth in relaxation time, even today there is intense dispute on the actual underlying mechanisms. Over the course of time many different theories have been put forward, such as, the entropy theory by Adams, Gibbs, and Di Marzio,[2,3] the coupling-model proposed by Ngai,[4] or the mode-coupling theory (MCT) by Götze and Sjögren.[5,6] The approach by which these theories explain the slowing down of the supercooled liquid with decreasing temperature, differs radically from case to case. In the entropy theory it is assumed, e.g., that the slowing down can be understood essentially from the thermodynamics of the system, whereas MCT puts forward the idea that at low temperatures the nonlinear feedback mechanisms in the microscopic dynamics of the particles become so strong that they lead to structural arrest of the system. The most successful theory has been MCT, which makes predictions that corroborate with experiments.

Recently, there has also been an increasing interest in the synthesis and self-assembly of polyhedral particles.[7–13] Much progress has been made in enumerating and characterizing the packing of polyhedral shapes and the self-assembly of polyhedral nanocrystals into ordered superstructures.[14] New synthetic methods give access to a wide range of well-defined polyhedral nanocrystalline shapes and faceted nano-particles including cubes, truncated cubes, cuboctahedra, truncated octahedra, and octahedra over a range of sizes from 100 to 300 nm.[15–24] The experimental realization of these particle shapes has sparked an effort to study their dynamics, densest crystal structures, and self-assembly.[25–27] de Graaf *et al.*[26] predicted the densest crystal structures of 145 convex polyhedra, whereas Glotzer *et al.*[25] studied the self-assembly of these polyhedra, starting from the isotropic fluid phase, and also found a quasi-crystalline phase of hard tetrahedra.[28]

[a]Electronic mail: n.tasios@uu.nl

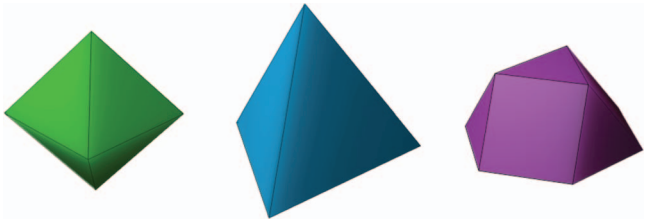

FIG. 1. The three particle shapes studied here. From left to right: octahedron, tetrahedron, and triangular cupola.

Advancements have also been made in the research of binary compounds of polyhedra by Escobedo *et al.*[29,30]

In what follows, we present the results of our study on the dynamics of convex polyhedral-shaped particles near the glass transition. The study was made using Monte Carlo (MC) simulations and the shapes investigated are octahedra, tetrahedra, and triangular cupola, depicted in Figure 1. The first two are Platonic solids, which are regular, convex polyhedra; the faces are congruent, regular polygons, with the same number of faces meeting at each vertex. Triangular cupola is a Johnson solid. We chose to study octahedra because they exhibit point symmetry. Tetrahedra on the other hand, while not being point-symmetric, exhibit a quasi-crystalline phase which can be readily suppressed by means of quenching.[28] This allows us to study the glass phase beyond this quasi-crystalline phase. Triangular cupola is the most asymmetric shaped particle studied here, and can be seen as half of a cuboctahedron, which is an Archimidean solid. In a recent study by Glotzer *et al.*,[25] triangular cupola did not exhibit any crystalline phases, which make it an interesting test case for the study of glass formation of polyhedral-shaped particles. Lower bounds for the packing fraction, ϕ_{LB}, of the densest known packings of these polyhedra have been estimated by de Graaf *et al.*[14] For triangular cupola, the packing fraction was estimated at $\phi_{LB} = 0.91836$, with a unit cell containing 2 particles. For tetrahedra, it was estimated at $\phi_{LB} = 0.85634$, with 4 particles in the unit cell, while for octahedra, $\phi_{LB} = 0.94736$, with 1 particle in the unit cell forming a Minkowski crystal.[27,31]

In Sec. II, we describe the simulation methods used and we present and discuss the results in Sec. III.

II. METHODOLOGY

We consider hard polyhedral-shaped particles that interact solely through a hard-core potential. To study the dynamics of the glass transition of these systems, MC simulations are performed in the NVT and NPT ensembles, in which we fix the number of particles N, the temperature T, and the volume V or pressure P, respectively. The simulations consist of N such particles, confined in a cubic box, and subject to periodic boundary conditions.

We employed NPT simulations to generate the initial configurations by quenching the particles, using a high compression rate, to the desired packing fraction, thereby suppressing crystallization. NPT simulations were also used to measure the equations of state.

The compression rate was set to $\Delta P^* = 0.0256$ per 100 MC steps, where $P^* = \beta P V_p$, and V_p the volume of the particle. A MC step was defined as $N + 1$ MC trials consisting of $N/2$ translations, $N/2$ rotations, and 1 volume change.

While quenching the samples, the crystallization was monitored using the averaged bond orientational order parameter,[32–35] and the least crystallized samples were chosen for our NVT simulations. The complex vector q_{lm} for particle i is defined as

$$q_{lm}(i) = \frac{1}{N_b(i)} \sum_{j=1}^{N_b(i)} Y_{lm}(\theta_{ij}, \phi_{ij}), \tag{1}$$

where $N_b(i)$ is the number of neighbors of particle i, and Y_{lm} are the spherical harmonics. θ_{ij} and ϕ_{ij} are the polar and azimuthal angles of the bond formed by particles i and j. The spherical harmonics for a given value l (and $|m| \leq l$) form a $(2l + 1)$-dimensional representation of the rotational group $SO(3)$. This means that the $q_{lm}(i)$ corresponding to a particular representation are scrambled by rotating the external coordinate system.

Solid-like particles are identified as particles for which the number of bonds per particle $\xi(i)$ is at least ξ_c, where

$$\xi(i) = \sum_{j=1}^{N_b(i)} H[d_l(i, j) - d_c],$$

with H the Heaviside function, d_c the dot product cut-off, and

$$d_l(i, j) = \frac{\sum_{m=-l}^{l} \bar{q}_{lm}(i)\bar{q}^*_{lm}(j)}{\left(\sum_{m=-l}^{l} |\bar{q}_{lm}(i)|^2\right)^{1/2} \left(\sum_{m=-l}^{l} |\bar{q}_{lm}(j)|^2\right)^{1/2}},$$

which is normalized to 1. $\bar{q}_{lm}$ is the quantity in Eq. (1), averaged over the nearest neighbors,

$$\bar{q}_{lm}(i) = \frac{1}{\widetilde{N}_b(i)} \sum_{j=0}^{\widetilde{N}_b(i)} q_{lm}(j),$$

where j runs over all $N_b(i)$ nearest neighbors of particle i, including i itself.[35] Crystallinity can be then defined as the number fraction of solid-like particles.

In our simulations, we used $l = 6$, $\xi_c = 5$, $d_c = 0.3$, and considered particle neighbors at cutoff radius $1.2r_c$, where r_c is the position of the first peak of the radial distribution function, $g(r)$ (see Fig. 2). Triangular cupola and tetrahedra showed insignificant levels of crystallinity (<1%). For Octahedra, at high packing fractions, ϕ, we chose configurations with a maximum of 4% crystallinity for production.

For the actual study of the dynamics of the particles, NVT simulations were used at various packing fractions and configurations of 2000 particles, prepared using the aforementioned NPT quenching scheme. Up to 10^7 Monte Carlo steps and some 20 independent simulations were used in averaging the various quantities studied. For all particle shapes studied, crystallinity fluctuated around some mean value, with the exception of Octahedra, which for packing fractions

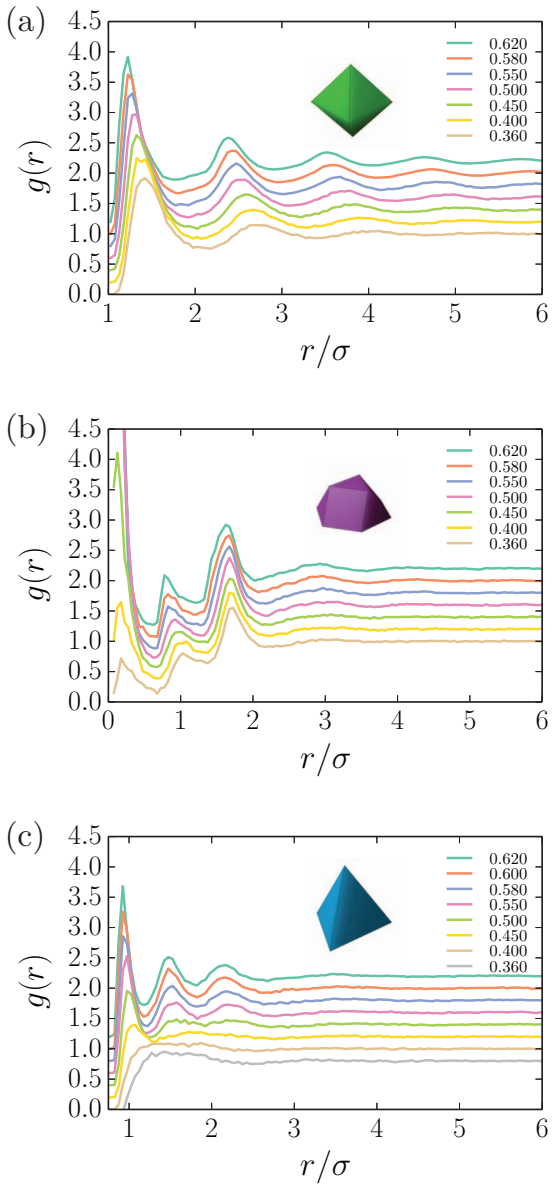

FIG. 2. Radial distribution functions, $g(r)$, of (a) octahedra, (b) triangular cupola, and (c) tetrahedra, for various packing fractions, ϕ, listed inside the figure. The distribution functions have been shifted by 0.2 in the vertical direction to make them distinguishable.

$\phi > 0.58$, could spontaneously crystallize. These configurations were not considered in our analysis.

The main quantity which was used in studying the slowing down of the relaxation near the glass transition, is the self-intermediate scattering function F_S (SISF), defined as

$$F_s(\mathbf{k}, t) = \frac{1}{N}\left\langle \sum_j e^{-i\mathbf{k}\left(\mathbf{r}_j(t_0+t)-\mathbf{r}_j(t_0)\right)} \right\rangle, \qquad (2)$$

where $\mathbf{r}_i(t)$ is the position of the centroid of particle i at time t (henceforth simply referred to as the particle position). For isotropic liquids, F_S is independent of the direction of the scattering vector $\mathbf{k}$ and depends only on its magnitude. This allows us to additionally average F_S over different directions and a small shell dk (similar to scattering experiments) of the wave vector. The self-intermediate scattering function is studied at wave vector k, close to the first peak of the static structure factor $S(k)$, which is relevant to the glass transition.[36]

It should be noted that, due to finite-size effects, the center of mass of the ensemble can drift away from its initial position. This is an unwanted situation since it introduces an unphysical collective motion of the particle ensemble. To account for this effect in our simulations, we kept track of the center of mass and extracted it from the particle positions.

When studying dynamics using Monte Carlo simulations, it is also important to choose an appropriate maximum displacement and orientation. We followed the scheme presented by Berthier and Kob,[37] which studied the behavior of the relaxation times, τ_α, for a range of different maximum displacements, to make an optimal choice.

Finally, the fragility of the glasses formed by the studied particle shapes was also investigated. Fragility characterizes how rapidly the structural relaxation time, τ_α, of a material slows down as it is cooled towards the glass transition temperature. Materials with higher fragility have a relatively narrow glass transition temperature range, while those with low fragility have a relatively broad glass transition temperature range.[38] In the case of colloidal glasses, fragility is often defined in terms of the sensitivity of τ_α with respect to the packing fraction, ϕ, instead of the temperature.[39,40] The concept of fragility is best summarized in a re-normalized Arrhenius plot (also referred to as an Angell plot[38,39]), where relaxation time, τ_α, is plotted as a function of the packing fraction rescaled by the packing fraction ϕ_g of the glass transition.

III. RESULTS AND DISCUSSION

Before studying the dynamics of the polyhedral-shaped particles, we investigated their structure briefly. In Figure 2, we have plotted the radial distribution function $g(r)$ vs r/σ, where $\sigma = V_p^{1/3}$ and V_p the volume of the particle. Octahedra exhibit structural correlations very similar to the ones observed for simple fluids, but for tetrahedra and triangular cupola, there are additional characteristics present. Upon increasing the packing fractions, tetrahedra show a splitting of the second peak and the appearance of a first peak at short distances, which is connected to the formation of icosahedra and pentagonal-dipyramids, signaling the transition to a more complex fluid, as indicated by the study of Glotzer *et al.*[28] Triangular cupola shows a very peculiar behavior, due to their asymmetric shape. The peak corresponding to distances close to zero (note that for triangular cupola, we define its centroid on its hexagonal face, bottom face as shown in Fig. 1) increases significantly with increasing packing fraction, as the number of particles that have their hexagonal faces aligned increases. At $r \approx 1.65\sigma$, a 3rd peak is observed; a consequence of particles aligning their peripheral faces.

In Figure 3, we show typical configurations of the three particle shapes in the isotropic phase. Here, it is evident that triangular cupola tends to form dimers, while tetrahedra create clusters of icosahedra and pentagonal-dipyramids.

As we mentioned in Sec. II, we followed the scheme presented by Berthier and Kob[37] to study the dependence of the relaxation time, τ_α, of the α-relaxation, on the maximum displacement. To this end, we calculated the SISF (Eq. (2)) and

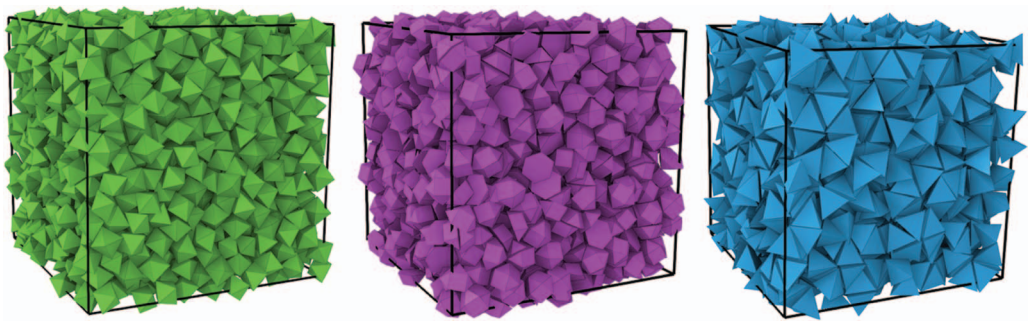

FIG. 3. Typical isotropic configurations of the three particle shapes studied. From left to right: Octahedra, triangular cupola, and tetrahedra are seen. Triangular cupola is observed to form dimers while tetrahedra create clusters of icosahedra and pentagonal-dipyramids.

fitted these with a stretched exponential $\sim e^{-(t/\tau_\alpha)^\beta}$ to extract the relaxation times τ_α. For each maximum displacement, we kept the rotational acceptance fixed at 30%. For convenience, we use the average acceptance ratio, $\bar{a}$, instead of the maximum displacement, which can easily be determined in a Monte Carlo simulation. In Figure 4, we show the relaxation time, τ_α, as a function of $\bar{a}$, for the three particle shapes at packing fraction $\phi = 0.62$ and additionally, $\phi = 0.55$ for octahedra. The curves have been normalized by their minimum value, τ_α^{min}, to get the maximum overlap. The plots exhibit a minimum plateau centered at $\bar{a} \approx 30\%$. Thus, for a remarkably large range of acceptance ratios, 5%–75%, similar relaxation time scaling is observed. It should be noted that we have observed that acceptance ratios for hard particles are quite low for relatively small maximum displacements when compared to other systems, like hard spheres and Lennard-Jones particle systems. This is to be expected and is a consequence of the particles' complex shape. It is remarkable, though, that we have a very strong agreement between the different particle shapes. As a result of this study, we chose to use an acceptance $\bar{a} = 30\%$ for the maximum displacement of our simulations. The average acceptance for the rotational trial moves was also kept at $\bar{a} = 30\%$. In Figure 5, we show the SISFs we extracted for the three particle shapes studied, where relaxation time was scaled by the short-time diffusion coefficient D_0. The SISFs were computed at a wave vector k close to the first peak of the static structure factor. For reference, we found $k\sigma = 5.6$, 3.83, and 4.9 for octahedra, tetrahedra, and triangular cupola, respectively. Triangular cupola exhibits no peculiarities, as expected, as it has no other phases except of the isotropic one.[25] We also

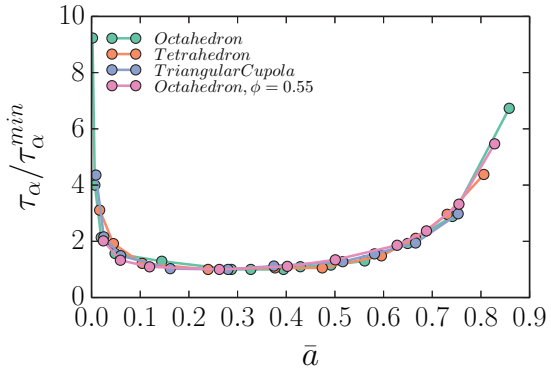

FIG. 4. Relaxation time τ_α, normalized by its minimum value, τ_α^{min}, vs the average acceptance ratio, $\bar{a}$, for the three particle shapes studied, at packing fraction $\phi = 0.62$ as well as $\phi = 0.55$ for octahedra. A plateau in the relaxation time is observed centered at $\bar{a} \approx 30\%$.

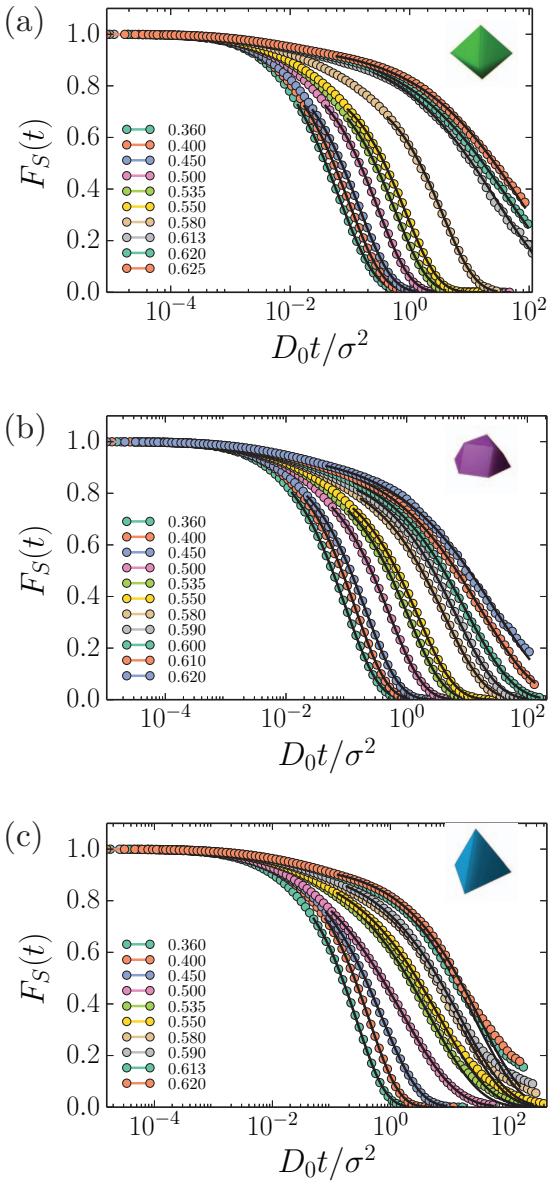

FIG. 5. The self-intermediate scattering function, $F_S(t)$, of (a) octahedra, (b) triangular cupola, and (c) tetrahedra, for varying packing fractions in the range $\phi \in [0.36, 0.62]$. Solid lines are stretched exponential fits of the α-relaxation part.

note that a plateau is not apparent in the SISF due to the short-time dynamics in MC simulations, which is different from the ballistic diffusion of other simulation schemes. Octahedra are known to exhibit two phases, a metastable body-centered cubic (BCC) phase and a Minkowski crystal.[27,31] In the packing fraction range $\phi \in [0.58, 0.60]$, all systems tend to crystallize into a Minkowski crystal before reaching the α-relaxation regime. After $\phi = 0.62$, octahedra do not crystallize very often, at least within the simulation time used here, but simulations of up to 10^8 MC steps seem to suggest that crystallization can still occur, but the nucleation times increase rapidly. At higher ϕ, a large slowing down of the relaxation time, in comparison with triangular cupola, is observed. Tetrahedra on the other hand exhibit a slightly different behavior, corresponding to the packing fraction at which a plateau is present in the equation of state (not shown here). The tails of the SISF are stretching for $\phi \geq 0.5$, which matches the packing fraction at which tetrahedra transition to a more complex fluid.[28] We were not able to discern with certainty whether the samples show any quasi-crystalline regions, as this requires a more elaborate characterization method. It is worth mentioning here, though, that diffraction patterns of dense configurations of tetrahedral-shaped particles show no (quasi-)crystalline order as there are no clear Bragg peaks visible. Fitting the relaxation with a stretched exponential, as indicated by the solid lines in Fig. 5, though, exhibited a deviation at the tail, a behavior which is not seen in regular supercooled liquids and is not explained by Mode Coupling Theory. We argue that this effect is due to the formation of clusters of pentagonal-dipyramids and icosahedra that was mentioned earlier. The clusters themselves, first need to break the cage formed by other clusters and individual particles, after which particles need to break the cage formed by particles from the same cluster. This was confirmed by means of visualization of the simulation runs; we monitored several clusters which seemed to slowly start moving and then breaking down to their individual constituents. It would be interesting in future work to somehow identify clusters and see how they diffuse before breaking apart.

By fitting the above self-intermediate scattering functions, Fig. 5, with a stretched exponential, we extracted the relaxation times, τ_α, for a wide range of packing fractions, ϕ. This allowed us to make an Arrhenius plot to study the fragility of the glass formed by the polyhedra we studied, similar to the work done by Mattsson *et al.*[40] For comparison, we also simulated and studied a polydisperse hard-sphere system with a size polydispersity of 10%. The Arrhenius plot can be seen in Fig. 6, where we have scaled the relaxation times with respect to that of spheres, so that in the limit of small packing fractions the four curves coincide. For ϕ_C, we chose the packing fraction at which the scaled relaxation time, $D_0\tau_\alpha/\sigma^2$, became equal to e^2. To describe the data, the Vogel-Fulcher-Tammann (VFT) equation was used, where the temperature was replaced by ϕ,

$$\tau_a = \tau_\infty \exp\left[\frac{A}{(\phi_c^{VFT} - \phi)^2}\right]. \quad (3)$$

We note that Eq. (3), unlike the regular VFT equation, uses the square of the packing fraction. As was reported in Ref. 41,

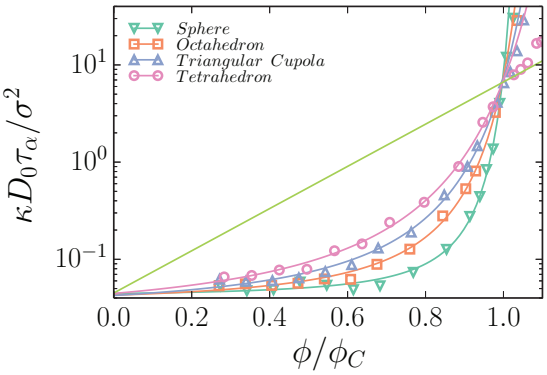

FIG. 6. Relaxation time τ_α (scaled by the short-time diffusion coefficient D_0) vs packing fraction for the three polyhedra and polydisperse hard-spheres. The relaxation times of the polyhedra are scaled by a dimensionless factor κ so that they fall on top of each other in the limit of small packing fractions. The lines are VFT fits of the data, while the green line is an indication of the limit of very strong glass formers.

we also find that this form offers a better fit of the relaxation data. ϕ_c^{VFT} sets the apparent divergence of the relaxation time. Moreover, free volume arguments[42] lead to the identification $\phi_c^{VFT} \equiv \phi_{rcp}$, the random close packing fraction where osmotic pressure diverges. Kinetic arrest must occur at ϕ_{rcp}, because all particles block each other at that density.[43–45]

From Fig. 6, it can be seen that the fragility (i.e., the slope of the curves) varies continuously from strong to fragile. Close to the glass transition, spheres appear to be the most fragile, followed by octahedra and triangular cupola, and tetrahedra being the stronger glass former.

The data were fit by both the VFT function (Eq. (3)) and the MCT power law, namely, $\tau_\alpha \propto (\phi_c^{MCT} - \phi)^{-\gamma}$. ϕ_c^{MCT} is predicted by MCT as the packing fraction at which the system becomes kinetically arrested to a nonergodic phase, whereas the system is still ergodic and liquid. The MCT expression gave a sufficiently good fit for packing fractions $\phi \lesssim 0.58$, while the VFT equation fits for packing fractions $\phi \gtrsim 0.58$. The results of the fits for all three particles are summarized in Table I. From the table, we also observe that the ergodic-nonergodic transition predicted by the VFT expression, indeed lies at higher packing fractions than the ones obtained by the MCT fits and the packing fractions that we investigated. Similar results were found in Refs. 41 and 46 for

TABLE I. VFT and MCT power law fitting parameters. ϕ_c^{MCT} is the ergodic-nonergodic transition critical packing fraction predicted by MCT, while ϕ_c^{VFT} is a packing fraction extracted from fitting with the VFT expression, and sets the apparent divergence of the relaxation time. The VFT parameter A controls the growth of the relaxation time as the packing fraction approaches ϕ_c^{VFT}.

	Fitting parameters			
Name	ϕ_c^{MCT}	ϕ_c^{VFT}	γ	A
Sphere	0.591908	0.657293	1.69861	0.0272889
Octahedron	0.603741	0.731188	1.69448	0.103722
Triangular cupola	0.595553	0.791872	1.68653	0.224292
Tetrahedron	0.575995	0.832166	1.67706	0.402016

colloidal spheres. It should be also noted that tetrahedra have a larger error bar due to their peculiar behavior. The critical exponent for spheres, γ, is slightly less than previously reported values,[46–48] $\gamma \in [1.7, 2.5]$. However, we mention here that γ is extremely sensitive to the precise range that is used in the MCT fitting as also noted in Refs. 46–48.

IV. CONCLUSIONS

In conclusion, we performed Monte Carlo simulations on pure systems of polyhedral-shaped particles and observed the formation of glassy phases without the introduction of size polydispersity. Polyhedra tend to align their facets, forming locally ordered structures which can hinder the formation of a crystal, in the case they are incommensurate with the stable crystal structure. In the case of octahedra the relatively small facets[49] allow for rearrangements which make it difficult to avoid crystallization in the packing fraction range $\phi \in [0.58, 0.62]$.

In addition, we presented a Monte Carlo scheme for analyzing the dynamics of the glass phase. We find rich behavior compared to simpler systems in which the particles interact with isotropic pair potentials. In the case of tetrahedra and triangular cupola, we observed locally ordered clusters which introduce additional relaxation modes that cannot be accounted for by conventional theories. Finally, we analyzed the fragility of the three polyhedra by making an Arrhenius plot of the α-relaxation times as obtained from fitting the SISFs with a stretched exponential.

Relaxation times as a function of packing fraction were also fitted by the MCT power law expression, and we found that the ergodic-nonergodic critical packing fraction, $\phi_c^{MCT} \in [0.57, 0.6]$, does not strongly depend on particle shape. In addition, the plot seems to indicate that polyhedra are stronger glass formers than systems of polydisperse hard spheres. Octahedra, which are point symmetric and crystallize relatively easily into a crystal with one particle in the unit cell, were found to be the most fragile of the particle shapes that we studied. Triangular cupola, which are not point symmetric and should crystallize in a crystal with two particles in the unit cell, forms dimer clusters and is slightly stronger glass former in comparison with octahedra and spheres. Finally, tetrahedra are the strongest glass formers, of the shapes studied here, as they possess large facets and form clusters of icosahedra and pentagonal-dipyramids in the fluid phase, which are incompatible with the stable crystal structure consisting of 4 particles in the unit cell.

It is tempting to speculate that one can identify polyhedra that are strong glass formers by assessing the size of the largest facet of a particle, whether or not the particle is point-symmetric, and the tendency to form locally favored clusters which are incompatible with the stable crystal structure. As an example, cubes do not form a glassy phase; although the facets are relatively large compared to the total surface area, cubes are point symmetric and form local clusters that coincide with the stable, simple cubic crystal structure. In any case, a larger variety of polyhedral shapes should be studied to draw any definite conclusions.

ACKNOWLEDGMENTS

N.T. and M.D. acknowledge financial support from a NWO-CW echo grant, and A.P.G. and M.D. from a NWO-VICI grant.

[1] R. Zallen, *The Physics of Amorphous Solids* (John Wiley & Sons, 1998).
[2] G. Adam and J. H. Gibbs, J. Chem. Phys. **43**, 139 (1965).
[3] J. H. Gibbs and E. A. DiMarzio, J. Chem. Phys. **28**, 373 (1958).
[4] K. L. Ngai, J. Phys. **2**, 61 (1992).
[5] W. Götze, *Liquids, Freezing and the Glass Transition: Part I (Les Houches Summer School Proceedings)* (North-Holland, 1991), p. 287.
[6] W. Götze and L. Sjögren, Rep. Prog. Phys. **55**, 241 (1992).
[7] J. Henzie, M. Grünwald, A. Widmer-Cooper, P. L. Geissler, and P. Yang, Nat. Mater. **11**, 131 (2012).
[8] J. Zhang, Z. Luo, B. Martens, Z. Quan, A. Kumbhar, N. Porter, Y. Wang, D.-M. Smilgies, and J. Fang, J. Am. Chem. Soc. **134**, 14043 (2012).
[9] M. Eguchi, D. Mitsui, H.-L. Wu, R. Sato, and T. Teranishi, Langmuir **28**, 9021 (2012).
[10] Z. Quan, W. Siu Loc, C. Lin, Z. Luo, K. Yang, Y. Wang, H. Wang, Z. Wang, and J. Fang, Nano Lett. **12**, 4409 (2012).
[11] J. J. Choi, K. Bian, W. J. Baumgardner, D.-M. Smilgies, and T. Hanrath, Nano Lett. **12**, 4791 (2012).
[12] Y. Zhang, F. Lu, D. van der Lelie, and O. Gang, Phys. Rev. Lett. **107**, 135701 (2011).
[13] L. Rossi, S. Sacanna, W. T. M. Irvine, P. M. Chaikin, D. J. Pine, and A. P. Philipse, Soft Matter **7**, 4139 (2011).
[14] J. de Graaf, L. Filion, M. Marechal, R. van Roij, and M. Dijkstra, J. Chem. Phys. **137**, 214101 (2012).
[15] A. R. Tao, D. P. Ceperley, P. Sinsermsuksakul, A. R. Neureuther, and P. Yang, Nano Lett. **8**, 4033 (2008).
[16] A. Tao, P. Sinsermsuksakul, and P. Yang, Angew. Chem., Int. Ed. **45**, 4597 (2006).
[17] Y. Sun and Y. Xia, Science **298**, 2176 (2002).
[18] E. Matijevic, Acc. Chem. Res. **14**, 22 (1981).
[19] X. Xia and Y. Xia, Nano Lett. **12**, 6038 (2012).
[20] B. Wiley, T. Herricks, Y. Sun, and Y. Xia, Nano Lett. **4**, 1733 (2004).
[21] A. S. Barnard, X. M. Lin, and L. A. Curtiss, J. Phys. Chem. B **109**, 24465 (2005).
[22] X. Zhang, C. Dong, J. Zapien, S. Ismathullakhan, Z. Kang, J. Jie, X. Zhang, J. Chang, C.-S. Lee, and S.-T. Lee, Angew. Chem., Int. Ed. **48**, 9121 (2009).
[23] H.-L. Wu, C.-H. Kuo, and M. H. Huang, Langmuir **26**, 12307 (2010).
[24] M. J. Solomon and S. C. Glotzer, Nat. Mater. **6**, 557 (2007).
[25] P. F. Damasceno, M. Engel, and S. C. Glotzer, Science **337**, 453 (2012).
[26] J. de Graaf, R. van Roij, and M. Dijkstra, Phys. Rev. Lett. **107**, 155501 (2011).
[27] S. Torquato and Y. Jiao, Nature **460**, 876 (2009).
[28] A. Haji-Akbari, M. Engel, A. S. Keys, X. Zheng, R. G. Petschek, P. Palffy-Muhoray, and S. C. Glotzer, Nature **462**, 773 (2009).
[29] M. R. Khadilkar and F. A. Escobedo, J. Chem. Phys. **137**, 194907 (2012).
[30] M. R. Khadilkar, U. Agarwal, and F. A. Escobedo, Soft Matter **9**, 11557 (2013).
[31] R. Ni, A. P. Gantapara, J. de Graaf, R. van Roij, and M. Dijkstra, Soft Matter **8**, 8826 (2012).
[32] P. J. Steinhardt, D. R. Nelson, and M. Ronchetti, Phys. Rev. B **28**, 784 (1983).
[33] P. R. ten Wolde, M. J. Ruiz-Montero, and D. Frenkel, Phys. Rev. Lett. **75**, 2714 (1995).
[34] P. R. ten Wolde, M. J. Ruiz-Montero, and D. Frenkel, J. Chem. Phys. **104**, 9932 (1996).
[35] W. Lechner and C. Dellago, J. Chem. Phys. **129**, 114707 (2008).
[36] U. Bengtzelius, W. Götze, and A. Sjolander, J. Phys. C: Solid State Phys. **17**, 5915 (1984).
[37] L. Berthier and W. Kob, J. Phys.: Condens. Matter **19**, 205130 (2007).
[38] C. A. Angell, Science **267**, 1924 (1995).
[39] C. A. Angell, K. L. Ngai, G. B. McKenna, P. F. McMillan, and S. W. Martin, J. Appl. Phys. **88**, 3113 (2000).
[40] J. Mattsson, H. M. Wyss, A. Fernandez-Nieves, K. Miyazaki, Z. Hu, D. R. Reichman, and D. A. Weitz, Nature **462**, 83 (2009).
[41] G. Brambilla, D. El Masri, M. Pierno, L. Berthier, L. Cipelletti, G. Petekidis, and A. B. Schofield, Phys. Rev. Lett. **102**, 085703 (2009).
[42] M. H. Cohen and D. Turnbull, J. Chem. Phys. **31**, 1164 (1959).

[43]K. S. Schweizer, J. Chem. Phys. **127**, 164506 (2007).
[44]S. Torquato, T. M. Truskett, and P. G. Debenedetti, Phys. Rev. Lett. **84**, 2064 (2000).
[45]C. S. O'Hern, S. A. Langer, A. J. Liu, and S. R. Nagel, Phys. Rev. Lett. **88**, 075507 (2002).
[46]R. Ni, M. A. Cohen Stuart, and M. Dijkstra, Nat. Commun. **4**, 2704 (2013).
[47]S. K. Kumar, G. Szamel, and J. F. Douglas, J. Chem. Phys. **124**, 214501 (2006).
[48]T. Voigtmann, A. M. Puertas, and M. Fuchs, Phys. Rev. E **70**, 061506 (2004).
[49]G. van Anders, N. K. Ahmed, R. Smith, M. Engel, and S. C. Glotzer, ACS Nano **8**, 931 (2014).